VOL. 80, NO. 26 JOURNAL OF GEOPHYSICAL RESEARCH SEPTEMBER 10, 1975

Heat Flow Through the Southern California Borderland

TIEN-CHANG LEE[1] AND THOMAS L. HENYEY

Department of Geological Sciences, University of Southern California
Los Angeles, California 90007

Fifty three new heat flow measurements together with 16 published data indicate that the heat flow (average of best values equals 1.74 μcal/cm^2 s) through basins of the southern California borderland is intermediate between heat flows through the Sierra Nevada and the Basin and Range provinces. In general, geothermal gradients in the borderland decrease with depth in the sediments, corresponding to an increase in thermal conductivity of 2–3% per meter. Owing to rapid sedimentation, surface heat fluxes may be locally masked from their steady state values by as much as 30%. Topographic corrections are usually less than 5%. Seasonal bottom water temperature variations are insignificant, but long-term climatic change in the last 37,000 yr may have reduced the gradient by 2–3%. Anomalous values were found in close proximity to turbidity current channels. The heat flow distribution shows two significant geographic trends. First, heat flows increase systematically southeastward in response to a late Cenozoic southeastward-migrating triple junction. Second, heat flows increase slightly toward the continent, suggesting that the offshore basins were formed progressively landward. In specific basins the measured values are uniform (standard deviation $\leq$ 0.1 HFU, where 1 HFU = 1 μcal cm^{-2} s^{-1}), but in other basins, only the corrected values are uniform. In the Santa Cruz Basin the corrected values are dominated by a north-south linear trend.

INTRODUCTION

The region between the mainland shoreline and the continental slope off southern California and northern Baja California (Figure 1) has been named the Continental Borderland for its distinctive basin and ridge topography [*Shepard and Emery*, 1941]. On the basis of bathymetry the borderland has been divided into northern and southern parts, separated by the inferred east-west-trending Santo Tomas fault [*Krause*, 1965]. This study represents heat flow data collected from the northern borderland.

The rock types forming the basement of the borderland are not well known, although it is one of the most extensively studied continental margins in the world [e.g., *Emery*, 1960; *Moore*, 1969]. The absence of granitic rocks in the dredge hauls and the presence of facies equivalent to the Franciscan group atop islands and banks have led to the belief that the borderland south of the Channel Islands is underlain by Franciscan basement [*Hill*, 1971]. The area north of and including the Channel Islands exhibits a predominantly ENW structural grain, which suggests that it is part of the Transverse Range province and hence is presumably underlain by Precambrian and Cretaceous plutonic rocks. The area south of the Channel Islands is dominated by a northwest structural pattern, similar to the adjacent onshore Peninsular Ranges. However, the Peninsular Range province including the Los Angeles Basin is underlain by a Cretaceous batholithic basement [*Yerkes et al.*, 1965; *Jahns*, 1954]. To the west of the borderland the Pacific Ocean floor is characterized by abundant Cenozoic volcanoes [*Menard*, 1955]. According to the magnetic anomaly patterns [*Atwater*, 1970], the oceanic floor adjacent to the borderland ranges in age from 25 m.y. at the northern end to 15 m.y. at the southern end.

The purpose of this study was to determine whether heat flow patterns on the borderland were consistent with tectonic models of the evolution of the western United States. The long thermal time constant of crustal rocks preserves a record of crustal and upper mantle events far into the geologic past; kilometers are scaled into millions of years. Thus the heat flow distribution depends on the long-term thermal history and hence serves as a contraint on tectonic modeling.

METHOD

Geothermal gradients were measured with outrigger thermistor probes spaced 1 m apart along a 6.4-m core barrel. Sediment temperatures were recorded in reference to the absolutely recorded bottom water temperature on a galvanometric film recorder modified from the type described by *Langseth* [1965]. Thermal conductivity was measured in the laboratory at 10- or 15-cm-depth intervals along each core by using the needle probe technique [*Von Herzen and Maxwell*, 1959] and was corrected for in situ temperature and pressure [*Ratcliffe*, 1960]. An interval heat flow was obtained from the gradient and the average thermal resistivity over the same depth interval. The average of the interval heat flows is taken as the heat flow at a given station. The standard error of a given heat flow measurement is between 10 and 14%; it is estimated from the standard error of the thermal resistivity at that station and the maximum likely error of ±8.5% for the interval gradients.

RESULTS

The results of 53 new heat flow measurements are listed in Table 1. Four measurements made on the continental shelf off central California are also given. These values are plotted to the nearest 0.1 μcal/cm^2 s (the heat flow units will henceforth be omitted for convenience) in Figure 2 along with the existing data of *Foster* [1962], *Von Herzen* [1964], and R. Anderson and L. A. Lawver (personal communication, 1973) in the borderland and *Henyey and Wasserburg* [1971] and *Sass et al.* [1971] in southern Calfornia.

Heat flow data in the northern borderland are unimodally distributed (Figure 3) with a range from 1.1 to 3.8. About 34% of the data lie within the mode of 1.6–1.8. Values higher than 2.8 (6%) are excluded from the frequency and cumulative curves which are dervied from a histogram drawn at an interval of 0.2 because they are very likely the result of local perturbations to be discussed later.

---

[1] Now at Department of Earth Sciences, University of California, Riverside, California 92502.

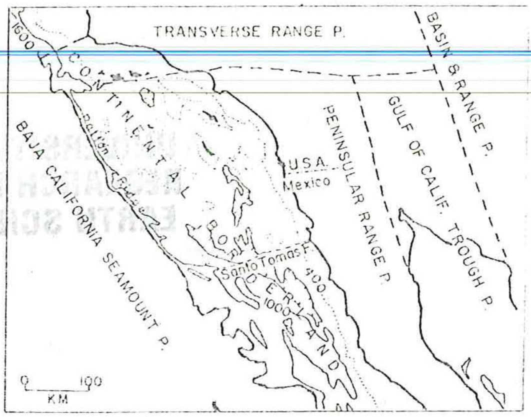

Fig. 1. Continental Borderland and adjoining physiographic provinces [after *Moore*, 1969]. Bathymetry is in fathoms (1 fm = 1.8288 m). Dashed curves are physiographic boundaries.

In general, the interval gradients decrease slightly with depth, corresponding to an increase in conductivity. As an example, sediment temperature profiles in the San Clemente Basin are shown in Figure 4. For profiles in other basins the readers are referred to *Lee* [1973].

Thermal conductivities of all core samples range between 1.5 and 2.6 μcal/cm² s °C, more than 85% of the values falling within the range of 1.7–2.0 μcal/cm² s °C. The standard deviation in each core lies between 2 and 8%. Generally, the conductivity increases 2–3% per meter from the top to the bottom of the core, probably as a result of sediment compaction. Abrupt variations in conductivity with depth are observed in the inner basins, San Pedro Basin, Santa Catalina Basin, and San Diego Trough, where the turbidite constituents of the sediments are higher than those in the outer basins. Two contrasting relations of conductivity versus depth are shown, for example, in Figure 5. The variations in thermal conductivity indicate the need to make ample measurements of conductivity of near-

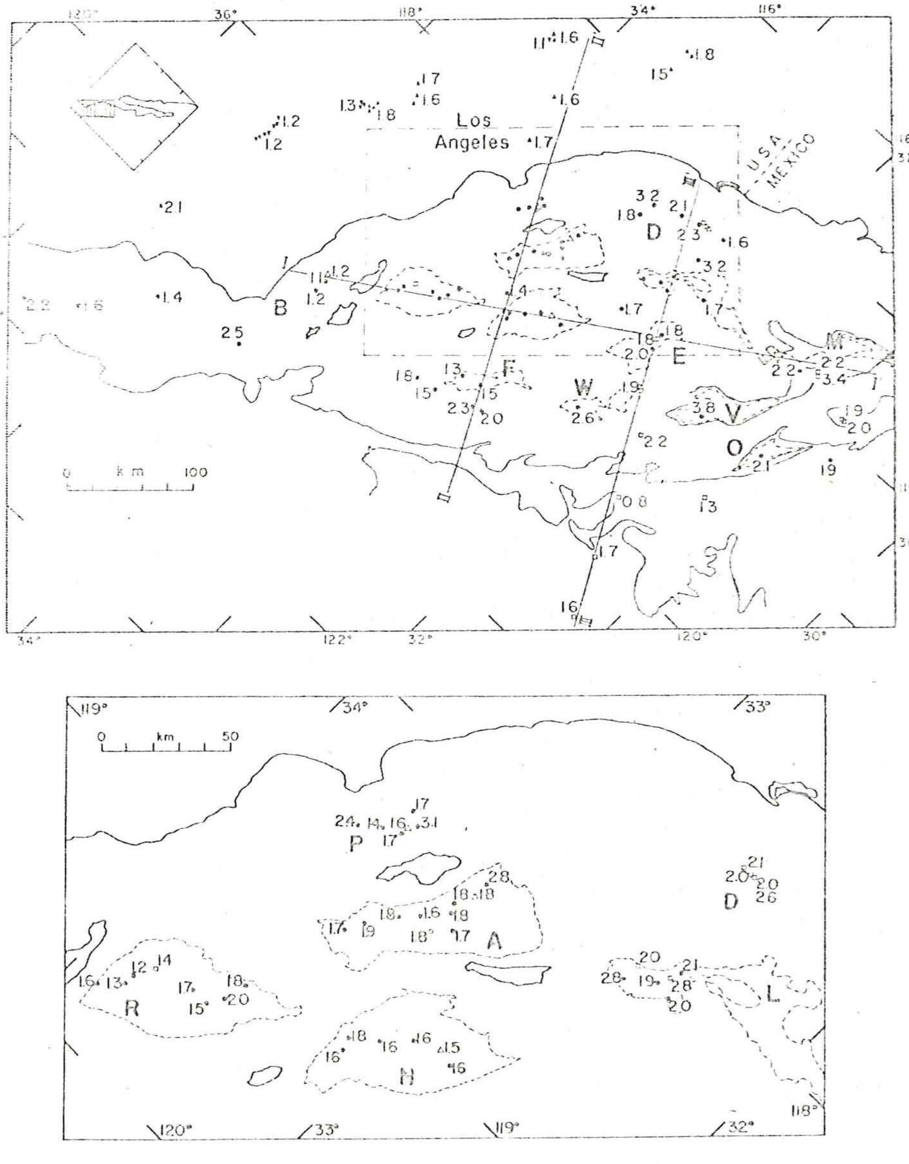

Fig. 2. Heat flow data from northern Borderland (including published data). Lines I-I', II-II', and III-III' are heat flow profiles shown in Figures 7, 8, and 9, respectively. The region boxed with dashed lines in the upper figure is enlarged in the lower figure. The offshore basins are indicated by A, Santa Catalina Basin; B, Santa Barbara Basin; D, San Diego Trough; E, East Cortes Basin; L, San Clemente Basin; M, Animal Basin; N, San Nicolas Basin; O, Outer Basin; P, San Pedro Basin; R, Santa Cruz Basin; V, Velero Basin; and W, West Cortes Basin.

TABLE 1. Heat Flow From the Southern California Borderland

	Location		Water Depth, m	Penetration, m	Water Temperature, °C	Gradient, °C/km	Conductivity, m cal/cm s °C	q	q_t	q_{ts}
[illegible]	N Lat.	W Long.								
					San Diego Trough					
[illegible]	32°24′	117°30′	1190	4.2 (4)	3.38	86 ± 11	(1.90)	1.63 ± 0.19	1.56	2.36
[illegible]	32°36′	117°33′	1145	5.3 (5)	3.61	120 ± 8	1.90	2.30 ± 0.21	2.24	3.40
[illegible]	32°44′	117°36′	1040	4.1 (5)	3.77	109 ± 8	1.94	2.12 ± 0.25	2.05	3.10
[illegible]	32°56′	117°42′	970	3.5 (4)	4.01	171 ± 16	1.90	3.24 ± 0.38	3.15	4.91
[illegible]	32°57′	117°50′	1050	4.0 (4)	3.98	92 ± 10	1.82	1.81 ± 0.23	1.75	2.65
					San Pedro Basin					
[illegible]	32°29′	118°20′	840	5.1 (5)	4.79	162 ± 2	1.93	3.08 ± 0.30	2.94	3.32
[illegible]	33°30′	118°24′	870	5.0 (5)	5.03	89 ± 15	1.92	1.72 ± 0.18	1.65	1.76
[illegible]	33°32′	118°18′	824	5.0 (5)	. . .	84 ± 2	1.92	1.66 ± 0.21	1.60	1.79
[illegible]	33°34′	118°26′	860	3.9 (4)	. . .	75 ± 2	1.82	1.40 ± 0.14	1.37	1.83
[illegible]	33°38′	118°30′	836	5.0 (5)	5.46	117 ± 2	2.02	2.36 ± 0.24	2.32	2.60
					San Clemente Basin					
[illegible]	32°12′	117°58′	1850	6.0 (5)	2.85	91 ± 6	(1.88)	1.71 ± 0.18	1.60	1.88
[illegible]	32°26′	117°46′	1490	5.0 (5)	3.04	172 ± 5	(1.88)	3.23 ± 0.35	3.08	3.08
[illegible]	32°26′	118°07′	1960	6.0 (5)	2.61	108 ± 4	1.83	2.00 ± 0.17	1.82	1.92
[illegible]	32°28′	118°00′	1830	4.7 (5)	2.60	109 ± 8	1.86	2.06 ± 0.18	1.91	2.01
[illegible]	32°30′	118°06′	1840	3.5 (4)	2.60	98 ± 0	1.91	1.87 ± 0.20	1.78	1.87
[illegible]	32°36′	118°11′	1820	5.2 (5)	2.60	161 ± 13	1.85	2.82 ± 0.25	2.61	2.74
					Santa Catalina Basin					
M1	33°10′	118°18′	1090	4.5 (5)	4.11	155 ± 8	1.83	2.81 ± 0.27	2.76	3.07
M2	33°08′	118°32′	1200	2.5 (3)	4.08	102 ± 1	1.68	1.70 ± 0.16	1.68	1.87
M3	33°11′	118°29′	1100	5.0 (5)	4.06	87 ± 10	2.06	1.77 ± 0.19	1.77	1.97
M4	33°12′	118°27′	1180	4.0 (4)	4.08	96 ± 1	1.89	1.78 ± 0.17	1.75	1.94
M5	33°15′	118°37′	1270	4.5 (5)	4.02	89 ± 4	1.82	1.62 ± 0.16	1.60	1.78
M6	33°18′	118°39′	1250	5.5 (5)	4.13	92 ± 4	2.01	1.81 ± 0.24	1.77	1.97
M7	33°22′	118°46′	1250	4.5 (5)	4.01	104 ± 11	1.84	1.93 ± 0.20	1.85	2.05
M8	33°24′	118°51′	1250	3.8 (4)	4.02	87 ± 2	1.98	1.73 ± 0.17	1.68	1.87
					Santa Cruz Basin					
[illegible]	33°30′	119°18′	1500	4.5 (4)	4.36	96 ± 2	1.82	1.76 ± 0.15	1.47	1.47
[illegible]	33°31′	119°24′	1710	4.6 (5)	4.18	104 ± 3	1.87	1.95 ± 0.18	1.82	1.82
R3	33°33′	119°28′	1840	4.6 (4)	4.20	91 ± 5	1.71	1.53 ± 0.14	1.46	1.64
R4	33°37′	119°28′	1850	4.5 (5)	4.20	93 ± 4	1.81	1.68 ± 0.17	1.61	1.79
R5	33°48′	119°36′	1870	4.0 (5)	4.19	67 ± 13	(1.82)	1.22 ± 0.12	1.14	1.33
R6	33°48′	119°39′	1710	4.9 (3)	4.19	68 ± 9	1.82	1.26 ± 0.11	1.17	1.37
R7	33°52′	119°44′	1570	4.7 (5)	4.17	88 ± 5	1,83	1.58 ± 0.14	1.40	1.40
					San Nicolas Basin					
N1	32°34′	118°29′	1120	5.2 (5)	3.37	85 ± 9	1.96	1.74 ± 0.16	1.74	1.74
N2	32°48′	118°56′	1450	6.4 (5)	3.75	91 ± 10	1.77	1.62 ± 0.14	1.59	1.17
N3	32°57′	118°58′	1670	5.4 (5)	3.76	94 ± 5	1.75	1.64 ± 0.14	1.60	1.72
N4	33°02′	119°04′	1700	4.8 (5)	3.76	96 ± 6	1.72	1.64 ± 0.14	1.61	1.73
N5	33°06′	119°12′	1630	4.4 (4)	3.75	85 ± 8	1.85	1.58 ± 0.14	1.55	1.67
N6	33°07′	119°09′	1700	4.5 (5)	3.76	102 ± 8	1.80	1.84 ± 0.17	1.75	1.88
N7	33°14′	119°03′	1180	5.1 (1)	3.83	79 ± 11	1.82	1.44 ± 0.13	1.41	1.41
					Tanner Basin					
T1	32°46′	119°53′	1110	3.2 (4)	. . .	109 ± 2	(1.82)	1.99 ± 0.18	1.87	1.96
T2	32°49′	119°54′	1110	4.3 (5)	3.91	125 ± 3	(1.82)	2.27 ± 0.21	2.14	2.23
T3	32°54′	119°44′	1370	4.0 (5)	3.92	89 ± 6	(1.82)	1.63 ± 0.15	1.57	1.65
T4	33°02′	119°47′	1460	3.2 (4)	3.94	71 ± 7	1.82	1.30 ± 0.12	1.21	1.34
T5	33°06′	120°01′	1190	5.0 (5)	3.82	83 ± 6	1.82	1.51 ± 0.13	1.46	1.62
T6	33°16′	120°04′	1100	2.1 (2)	3.60	98 ± ?	(1.82)	1.78 ± 0.16	1.64	1.71
					Santa Barbara Basin					
B1	34°13′	120°88′	560	5.7 (5)	6.47	63 ± 7	1.63	1.12 ± 0.11	1.12	1.72
B2	34°14′	120°08′	560	5.7 (5)	6.40	69 ± 11	1.74	1.20 ± 0.11	1.20	1.84
					East Cortes Basin					
E1	32°13′	118°38′	1630	5.0 (3)	. . .	112 ± 6	1.81	2.05 ± 0.18	1.97	2.16
E2	32°15′	118°24′	1500	6.0 (5)	3.22	98 ± 5	(1.81)	1.77 ± 0.15	1.72	1.89
					Miscellaneous Location					
M1	30°45′	118°11′	2470	4.1 (4)	. . .	101 ± 3	1.89	1.90 ± 0.18	. . .	. . .
M2	31°07′	118°33′	2150	4.2 (5)	. . .	113 ± 1	(1.84)	2.08 ± 0.19	. . .	. . .
M3	31°21′	117°50′	1970	3.0 (2)	. . .	117 ± ?	(1.89)	2.21 ± 0.20	. . .	. . .
M4	31°37′	118°40′	2330	4.2 (3)	. . .	207 ± 1	(1.84)	3.83 ± 0.35	. . .	. . .
M5	32°17′	119°18′	1740	3.1 (2)	. . .	141 ± ?	1.84	2.59 ± 0.24	. . .	. . .

TABLE 1. *(continued)*

Station	Location		Water Depth, m	Penetration, m	Water Temperature, °C	Gradient, °C/km	Conductivity, m cal/cm s °C	q	q_t	q_{ts}
	N Lat.	W Long.								
	Continental Shelf off Central California									
C1	34°20′	120°51′	790	4.5 (5)	4.50	130 ± 11	1.89	2.46 ± 0.22	2.45	. . .
C2	35°00′	121°02′	590	4.4 (3)	5.75	71 ± 6	1.98	1.42 ± 0.13	1.39	. . .
C3	35°22′	121°33′	970	5.5 (5)	4.78	70 ± 6	2.26	1.58 ± 0.10	1.57	. . .
C4	35°40′	121°49′	1010	4.5 (5)	. . .	108 ± 8	1.96	2.18 ± 0.19	2.16	. . .

Penetration is penetration of the lowermost probe, the numbers in parentheses expressing the number of probes used in calculation. Gradient is the average gradient with standard deviation. Conductivity is thermal conductivity; the numbers in parentheses are assumed values from a nearby station. The value q (in microcalories per centimeter square second) is the average of interval heat flows with standard error $q(a^2 + b^2)^{1/2}$, where a is an assumed error of 8.5% in gradient and b is the calculated standard error (in percent) of thermal resistivity. Value q_t is corrected for topography, and q_{ts} is corrected for topography and sedimentation.

shore sediments or of sediments in areas of extreme topographic relief where either rapid, variable, or sporadic sedimentation is likely.

PERTURBING FACTORS AFFECTING HEAT FLOW THROUGH THE BORDERLAND

The effects of topography, conductivity and heat generation contrasts, subsidence and uplift, sedimentation and erosion, temporal and spatial surface temperature variation, and interstitial water circulation are considered in this section.

Bottom water temperature. Variations in bottom water temperature arise from climatic change, change in oceanic circulation, annual surface water temperature fluctuation, and regional and local uplift or subsidence.

Below sill depths of basins on the borderland the seasonal fluctuation of bottom water is very likely negligible, since (1) the annual surface water temperature fluctuation (range 6°C) diminishes to a small value at a depth of 200 m [*Emery*, 1960, Figure 84], (2) the temperature gradients in the water column below sill depths are less than 10°C/km, and (3) the observed geothermal gradients do not reflect the curvature typical of annual bottom water temperature oscillations. The large volume of nearly isothermal water below sill depths serves to buffer annual surface water temperature fluctuations. However, an overturn period of 2 yr estimated from oxygen content in the bottom water [*Rittenberg et al.*, 1955] suggests that the bottom water may interact with shallow water with periods on this order or greater.

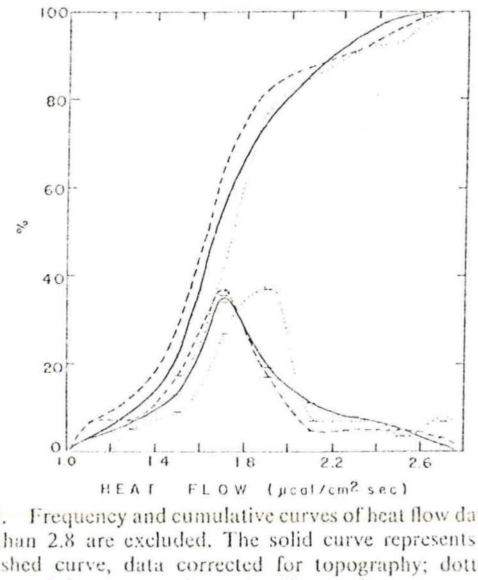

Fig. 3. Frequency and cumulative curves of heat flow data. Values greater than 2.8 are excluded. The solid curve represents observed data; dashed curve, data corrected for topography; dotted curve, data corrected for topography and sedimentation.

The California current over the outer borderland has been nearly constant in position and direction during the past 12,000 yr, as suggested from the generally uniform deposition of biogenic carbonates in Tanner Basin [*Gorsline et al.*, 1968]. The associated countercurrent over the inner borderland is probably steady also. Hence a significant change in bottom water temperature resulting from a major shift in circulation patterns should not be expected.

Turbidity currents which scour and fill may affect neighboring gradients. The presence of scour channels has been documented by *Moore* [1969] in the San Diego Trough, a basin which has been overfilled with sediments. Nine heat flow values measured in the trough yield a trimodal distribution (Table 1 and Figure 6). The two highest values (3.24 and 2.58) were located in the channels, whereas the two smallest values (1.63 and 1.81) were at channel edges. Three (2.30, 2.12, and 2.05) of the five intermediate values were measured at distance from the known channels. This correlation of heat flow with proximity to channel reflects the effects of microrelief (20–30 m) coupled with erosion and/or sedimentation. The remaining two intermediate values were also located within a channel and may reflect the fact that either the channel is no longer active or the effects of microrelief and erosion and/or sedimentation are balancing each other. A high heat flow near the southeastern end of Santa Catalina Basin may also have been affected by an active turbidity current channel, as suggested by the proposed routes of sediment transport in this area [*Emery*, 1960; *Moore*, 1969]. Apparent anomalous values at other stations on the borderland, particularly near the base of steep escarpments, may also be attributable in some cases to turbidity currents. Because the occurrences and effects of these processes are poorly known, they can only be considered to have contributed to the intrinsic scatter of the data.

Climatic change on the borderland during the 37,000 yr has been studied by *Gorsline and Barnes* [1972], using $^{18}O/^{16}O$ ratios in benthonic and planktonic foraminifera. Calculations based on the resultant paleotemperatures suggest that the measured geothermal gradient has been reduced by 2.6°C/km for 0.003 cm²/s (appendix), or about a 2–3% reduction in the undisturbed heat flow. This effect, which may vary from basin to basin, is probably smaller than the experimental error of the heat flow measurements.

Four heat flow measurements were made in relatively shallow waters on the continental shelf off central California where a basin and range structure is not present. They were located

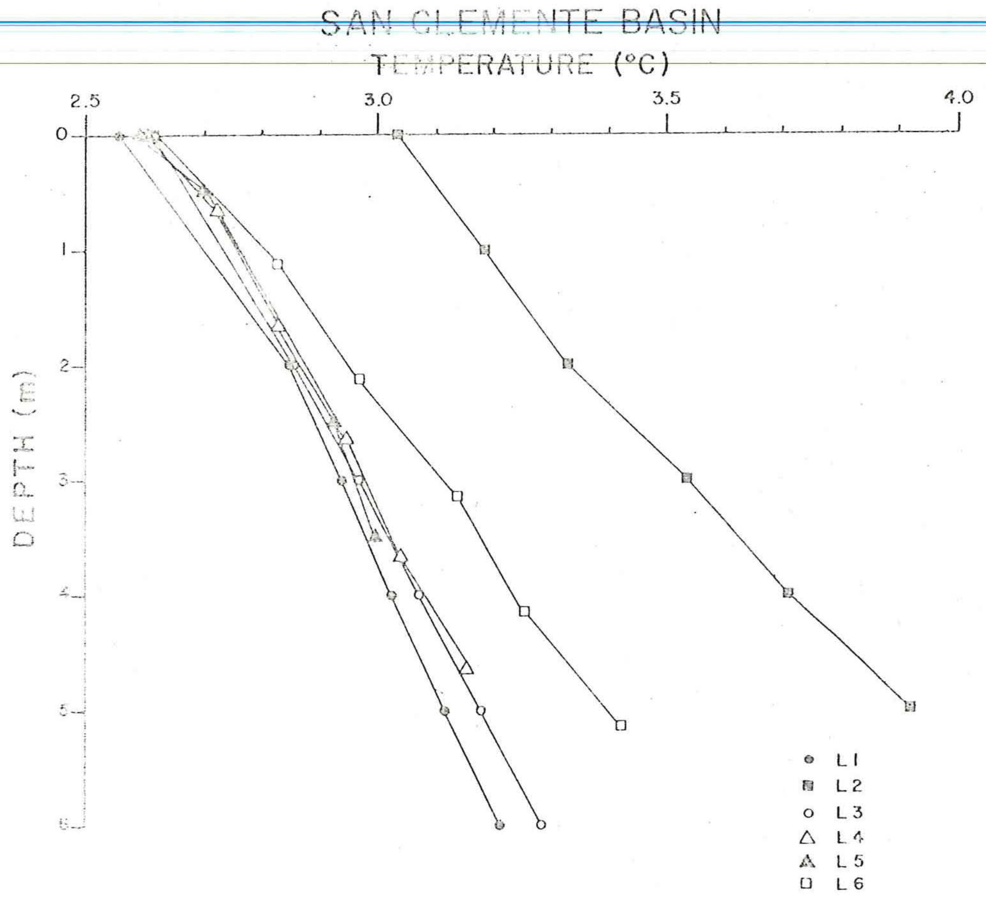

Fig. 4. Sediment temperature versus depth in San Clemente Basin.

within 40′ of an upwelling center which develops from March to July around 35°N [*Sverdrup et al.*, 1942]. Toward the end of summer the upwelling ceases gradually and evolves into a number of eddies through which the coastal and oceanic waters are interchanged, probably affecting water at all depths on the shelf. The stability of bottom water temperatures under such conditions is not known. The patterns of sediment transport and deposition are also poorly known in this area; apparent channels were noted at some localities. Hence the quality of these measurements must be regarded as inferior to those measured in the borderland.

Relief and conductivity contrast. *Birch*'s [1950] method of topographic correction has been applied to all heat flow measurements in the borderland, a steady state topography being assumed. An equivalent lapse rate of 1.5°C/km is used, the value of which is not crucial because of the shallow corer penetration. The relief within 30 km of a station is estimated from U.S. Coast and Geodetic Survey bathymetric charts with a scale of 1:250,000 and a contour interval of 50 m. The effect of microrelief such as channels and hummocky topography on the order of 50 m or less has been neglected for lack of detailed data. For the same reason the relief within 1 km of a station is also neglected. Warm rim effects are negligible because land is rarely within 30 km of a station; wherever it is, it subtends only a small solid angle. Under the assumption of uniform conductivity, corrections of −1 to −19% are applied; most corrections are less than 5%. Results of the topographic corrections are given in Table 1 (column q_t).

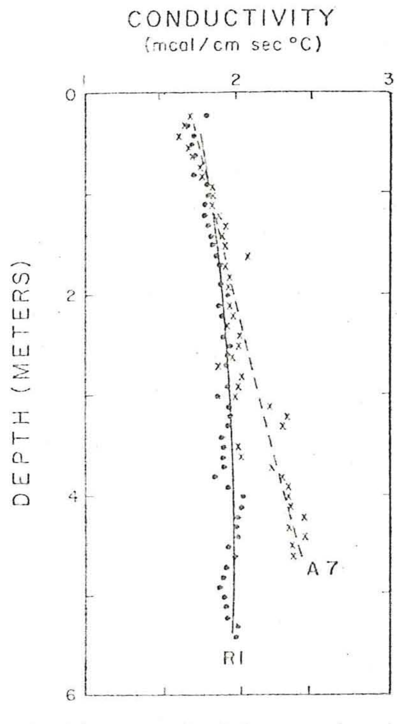

Fig. 5. Conductivity versus depth for two selected core samples. Solid and dashed curves are second degree polynomials fitted to data at stations R1 (Santa Cruz Basin) and A7 (Santa Catalina Basin), respectively.

Heat flow refraction due to nonhorizontal boundaries

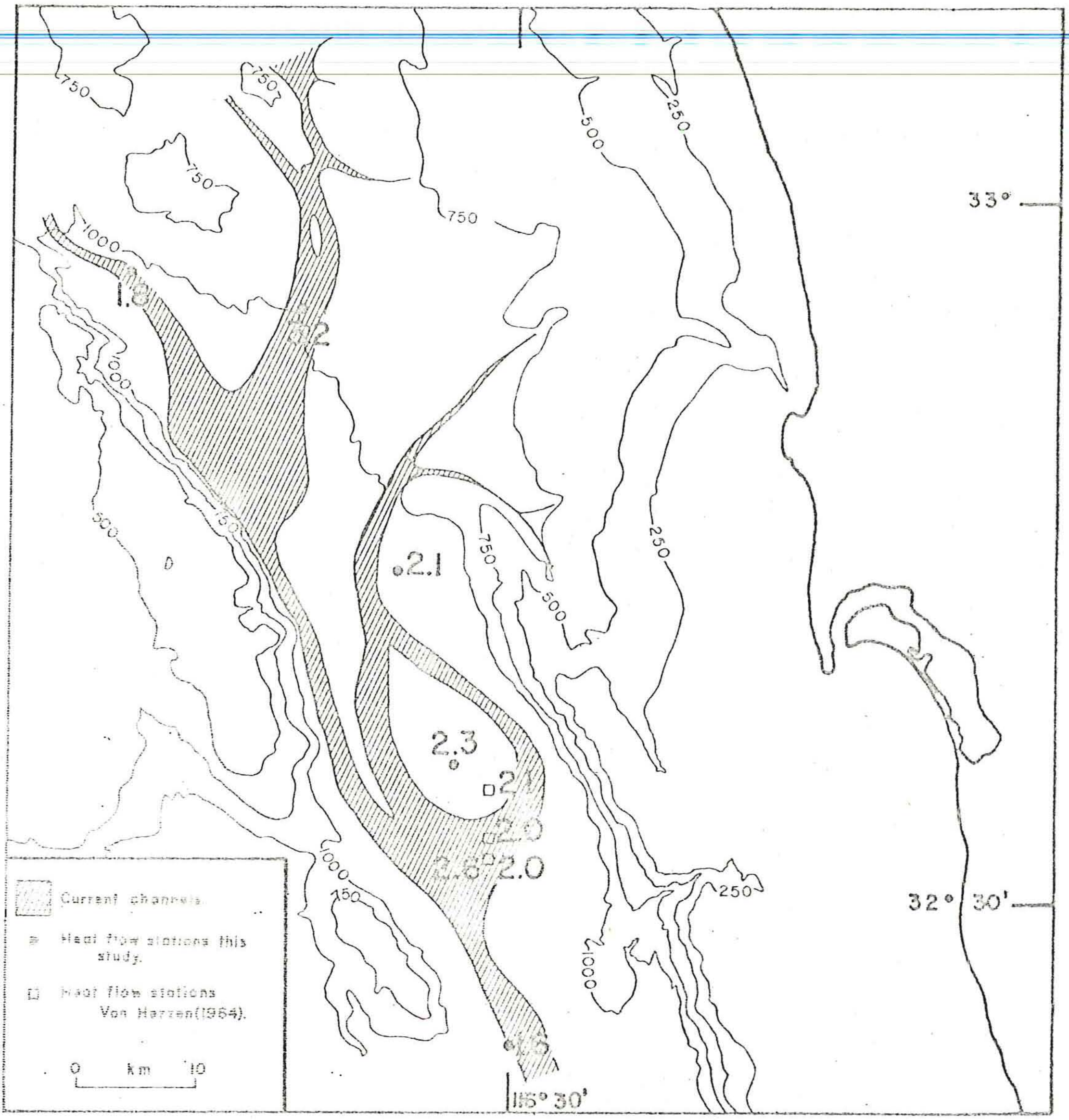

Fig. 6. Heat flow data distribution and turbidity current channels in San Diego Trough. Open square represents data from *Von Herzen* [1964]. Shaded areas are channels [*Moore*, 1969].

between dissimilar media can cause significant variation in the surface heat flow. For example, the relative heat flow across a sediment-bedrock contact may differ by as much as the corresponding conductivity ratio [*Lee*, 1973]. Because most stations were located at a large distance from bedrock outcrops, refraction effects are negligible. However, for the few stations located on basin slopes or in saddle regions where the sediments are thin, the refraction effects may be significant. Assuming a two-dimensional model, *Lee* [1973] used the finite element method to show that the net effect of conductivity contrast, relief, and spatial bottom water temperature variation expected for the borderland has probably reduced basin fluxes by an average of 5%.

Sedimentation. Thermal disturbances resulting from constant sedimentation rates and instantaneous slumping have been discussed by *Von Herzen and Uyeda* [1963], using a one-dimensional model. The transient geothermal gradient is always smaller than the steady state gradient, and measured heat flows are biased toward lower values. In general, sedimentation rates in the Continental Borderland increase northwestward and toward the continent. Locally, the rates change not only from basin to basin but also from point to point within a given basin. Temporal variations in rate are also expected in view of the unpredictable occurrence of turbidite deposits in the sedimentary column, as evidenced by the nonlinearity between age and depth of the sediments [*Emery and Bray*, 1962; *Inman and Goldberg*, 1963]. Furthermore, since the basins are believed to have formed progressively inland from Miocene to early Pleistocene [*Emery*, 1960], the depositional environment was probably drastically altered each time a new basin was formed. This leads to an uncertainty in the accumulation time and the extrapolation of sedimentation rates determined from piston cores.

Because sedimentation rates were not determined for the cores taken in this study, we have extrapolated the published data [*Emery and Bray*, 1962; *Gorsline et al.*, 1968]. The extrapolated rate was generally consistent with the rate estimated from the isopach map of *Moore* [1969] for the postorogenic sediments, a total accumulation time of 10^6 yr being assumed. A total accumulation time of 10^6 yr is also consistent with the average annual contribution of sediment from the southern California watershed [*Moore*, 1969]. Thus we have assumed this accumulation time for our calculations.

Based on equation (38) of *Jaeger* [1965], the sedimentation corrections vary from 2 to 47%, corresponding to a range of sedimentation rates from 50 to 110 cm/1000 yr at different stations, assuming a constant thermal diffusivity, 0.003 cm²/s. Results of topographic and sedimentation corrections are given in Table 1 (column q_{ts}).

Hydrothermal circulation. The geothermal isotherms are usually parallel or subparallel to the ground surface even in areas of significant relief. Thus on a given datum with respect to sea level, the temperature is generally greater below topographic highs than below topographic lows. As a result the density of water on this datum is less below topographic highs than below the topographic lows. If the permeability of the rocks is sufficiently large, hydrothermal circulation can occur. The circulation currents would rise beneath topographic highs and return at the topographic lows, the result being heat flows that are relatively higher over the ridges than in the basins.

A value of 3.23 (station L2) has been obtained from the northeastern basin slope of the San Clemente Basin. This station is in close proximity to the San Clemente fault [*Moore*, 1969], and the high value may be the result of hydrothermal circulation through the fault zone rather than through the interstices of the basement rocks. A measurement (1.68, station N1) in the saddle between San Clemente and San Nicolas Basin is similar to values in nearby basins. Another value (1.44, station N7) measured in the saddle between Santa Cruz and San Nicolas Basin is less than values in surrounding basins. Because the permeability of the basement rocks is poorly known and most of our measurements were made in the basins, the nature of hydrothermal circulation on the borderland remains unsolved.

DISCUSSION AND CONCLUSIONS

On the basis of 84 measurements which include 16 values from *Foster* [1962], *Von Herzen* [1964], and R. Anderson and L. A. Lawver (personal communication, 1973), uncorrected heat flows through the northern borderland average about 1.86.

Comparison with adjacent physiographic provinces indicates that this heat flow is significantly higher than that through the Sierra Nevada province [*Roy et al.*, 1968; *Sass et al.*, 1971] but less than that through the Basin and Range province [*Roy et al.*, 1968] and Gulf of California rift [*Lawver et al.*, 1973]. It is similar to fluxes through the Coast Ranges [*Sass et al.*, 1971]. Average heat flows in the Peninsular Ranges are not well established. Clearly, it would be more definitive to compare 'reduced heat flows' [*Roy et al.*, 1972] between these provinces; however, data on radioactivity on the borderland are lacking. Considering the likely crustal structure [*Shor and Raitt*, 1958] and the lithology [*Emery*, 1960; *Krause*, 1965; *Doyle*, 1973], the reduced heat flow is probably above average and similar to that of the Basin and Range province (i.e., 1.4 HFU, where 1 HFU = μcal cm^{-2} s^{-1}).

Topographic corrections reduce the average value on the borderland from 1.86 to 1.78, but the combined corrections for topography and sedimentation increase the average to 2.05 for best estimates of sedimentation rates as discussed earlier. These three values are presumably biased by the sampling distribution as well as disturbing effects. If the 'best' value from each basin is taken, the average is 1.74 for the measured values, 1.67 for the topographically corrected data, and 1.99 for the data corrected for both topography and sedimentation. Each best average falls within its modal values (Figure 3).

The empirical relation between heat flow and age of the Pacific Ocean floor [*Sclater and Francheteau*, 1970] yields a 20-m.y. age for sea floor with a 1.8 ~ 2.0 heat flow (borderland mean value). This age is compatible with the age of the adjacent deep sea floor (15–25 m.y.) as inferred from magnetic anomaly patterns [*Atwater*, 1970]. *Sclater and Francheteau* [1970] also proposed a similar empirical relationship between continental heat flow and age of the last thermal event for North America, but having almost one order of magnitude greater time decrement. According to the continental relationship the borderland mean is also consistent with the termination of the Mesozoic batholithic emplacement in California. Although the crust beneath the borderland is apparently continental in nature [*Shor and Raitt*, 1958], this region's proximity to the Pacific oceanic lithosphere cannot rule out, and may in fact require, oceanic thermal control. Thus although the mean borderland heat flow does not permit resolution of the age of the last tectonic or resultant thermal event, it is consistent with the regional tectonic pattern.

The uncorrected heat flow trend in a direction parallel to the strike of the regional structure (Figure 7, profile I-I') generally confirms *Von Herzen*'s [1964] conclusion drawn from a few sparsely spaced data points that heat flows decrease systematically northward in the borderland. Superimposed upon this trend is a maximum over the divide between the Santa Cruz and San Nicolas basins (Figures 2 and 7). The trend appears to correlate with increasing sedimentation rates to the north; the maximum occurs where thermal blanketing due to sediments is probably a minimum. As a result of the apparent correlation of heat flow with sedimentation, we have also plotted a heat flow profile along the same trend corrected for topography and sedimentation (Figure 7, dotted curve). As expected, these two curves converge to the southeast but diverge to the northwest. Differential sedimentation rates have significantly altered the characteristics of the heat flow trend from the Santa Cruz Basin across the Channel Islands to the

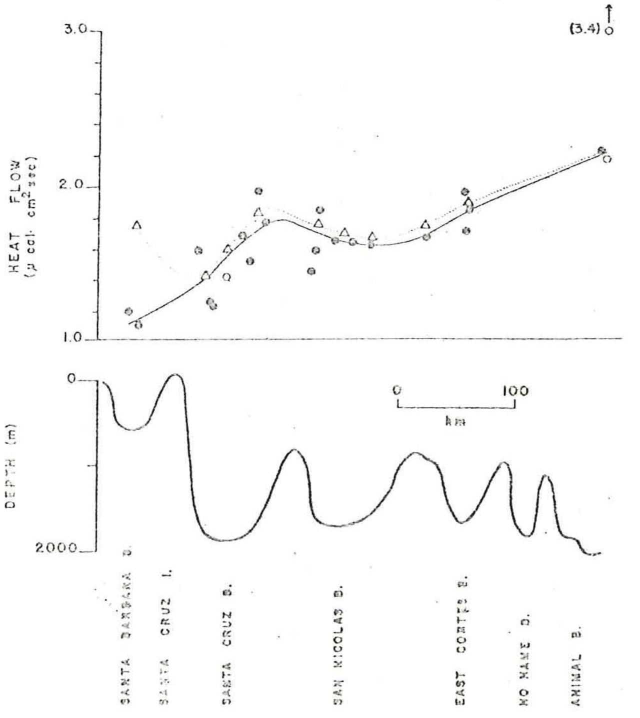

Fig. 7. Heat flow profile I-I' along the strike of regional structure. See Figure 2 for location. Solid curve shows trend of observed data projected within 30 km of the profile (solid and open circles); dotted curve shows trend of corrected average data (open triangles). Open circles are from *Von Herzen* [1964].

Santa Barbara Basin. The heat flow low is shifted from the Santa Barbara Basin to the Santa Cruz Basin in the 'corrected' profile and thus coincides with the structural transition from the northwesterly oriented Peninsular Range structure to the east-striking Transverse Range structure, or presumably with the basement transition from Franciscan to plutonic rocks.

Extending this profile further north or south cannot be done with confidence at present because of insufficient data. On the basis of a few measurements made by *Von Herzen* [1964] in the southern borderland, the linear heat flow trend between East Cortes and Animal basins does not continue to increase linearly to the southeast; however, the heat flows appear on the average to be higher in the southern than in the northern borderland. Thus to the first order the regional heat flows increase southeastward. Superimposed upon this regional trend are components with an apparent wavelength on the order of 75 km. Three measurements made on the continental shelf off central California suggest that heat flows may increase northward, north of the Transverse Ranges, although the significance of these values cannot be evaluated with confidence for lack of knowledge about disturbing environmental effects. Above-normal heat flows here would be consistent with similar values in the Coast Ranges [*Sass et al.*, 1971].

In an east-west direction across the borderland, heat flows appear to increase landward except for a possible maximum associated with a trough in the Patton Ridge system (Figures 1 and 8). However, this trend is less definite than the north-south trend. Landward from the shoreline, heat flows do not appear to show any significant trend [*Henyey and Wasserburg*, 1971; *Sass et al.*, 1971]. Thus the innermost basins, San Pedro Basin and San Diego Trough, appear to form a high heat flow zone, although the data are too scattered to show the magnitude and exact locality of the maximum. The average value of the corrected heat flow data in each basin is also plotted in Figure 8. The corrected and uncorrected data give essentially the same heat flow trend. In San Pedro Basin the highest value at station P1 is excluded from the average owing to the probability of local perturbation. About 180 km south of II-II′, a similar heat flow trend occurs also along profile III-III′ (Figure 9) which is approximately in line with profile I-I′ of *Von Herzen* [1964]. Heat flows through the Peninsular Range province on a landward extension of profile III-III′ are low to normal [*Roy et al.*, 1973], and hence it is likely that the San Diego Trough is an area of relatively high heat flow as stated earlier.

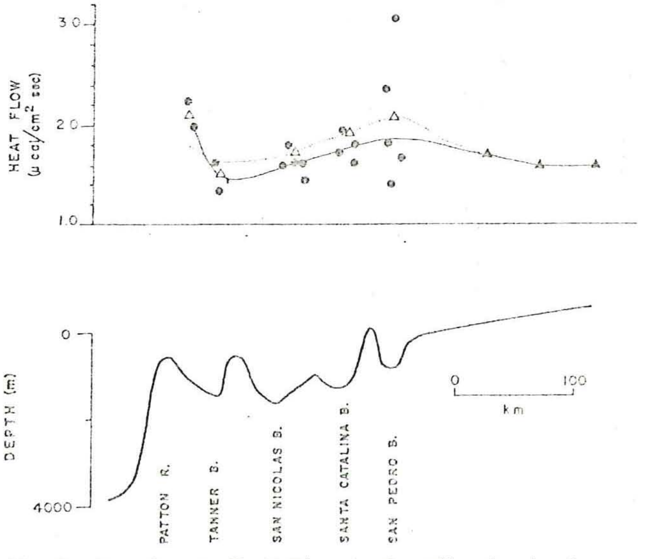

Fig. 8. Heat flow profile II-II′ across the strike of regional structure. See Figure 7 for caption. Solid triangles are from *Henyey and Wasserburg* [1971] and *Sass et al.* [1971].

Heat flows in Santa Catalina, San Nicolas, and Santa Barbara basins are generally uniform throughout the individual basins. The averages of uncorrected values are 1.75, 1.67, and 1.17 with standard deviations of 0.10 (9 values), 0.09 (6 values), and 0.05 (3 values), respectively. However, variations of up to a factor of 2 are found in the inner basins, San Pedro Basin, San Clemente Basin, and San Diego Trough. The variations can be attributed largely to effects of topography and sedimentation. Thus the corrected heat flows appear uniform except for Santa Cruz Basin, where the measured values are scattered and the corrected values show a linear heat flow trend from 1.8 at the south to 1.4 at the north over a distance of 60 km (Figure 7).

The landward increasing heat flow in the borderland may indicate that radioactivity in the crustal rocks increases toward the continent. An increase in radioactivity can result from either a change in lithology or a thickening of the crust overlying a uniform upper mantle. The increase of heat flow toward the southeast appears less likely to be related to a variation in radioactivity, considering the distribution of rock types described by *Emery* [1960], *Krause* [1965], *Doyle* [1973], and other workers.

Another explanation for a landward increase in heat flow follows a suggestion by *Lachenbruch and Sass* [1973] that heat flow anomalies in the California Coast Ranges may result from conversion of mechanical energy to heat along the broad shear boundary between the North American and Pacific plates. For borderland latitudes this boundary is probably represented by the following faults from west to east (Figure 10): San Clemente, Newport-Inglewood, Whittier-Elsinore, San Jacinto, and San Andreas. Only the San Clemente fault lies offshore, which, coupled with the fact that long-term strain rates probably increase eastward (reaching a maximum at the San Andreas fault), would imply a landward increase in heat flow. It is important to note, however, that *Henyey and Wasserberg* [1971] did not find evidence for a significant amount of mechanical to thermal energy conversion along the San Andreas fault in northern California. One explanation for this apparent paradox might be that thermomechanical energy conversion is an efficient process only in the lower portion of the lithosphere (depth greater than 20 km) where nonelastic slip (creep) occurs. Thus a broad anomaly would result and would be recognizable only by regional heat flow studies.

Alternatively, the borderland heat flow pattern may be interpreted as representing a transient thermal condition. Since regional heat flow has been shown to decrease with the age of the most recent regional tectonic activity or thermal event [*Sclater and Francheteau*, 1970], the landward increasing heat flow may reflect the progressive landward development of offshore basins [*Emery*, 1960; *Yeats*, 1968, *Yeats et al.*, 1974], while the southeastward increasing heat flow suggests that formation of the continental borderland proceeded from northwest to southeast. This suggestion is in agreement with the Cenozoic plate tectonic model proposed by *Atwater* [1970] for western North America, if we assume that the borderland resulted from the subduction of a segment of the East Pacific Rise (T. C. Lee, manuscript in preparation, 1975). If subduction proceeded southeastward and the ridge-trench-transform triple junction was equivalent to a southeastward

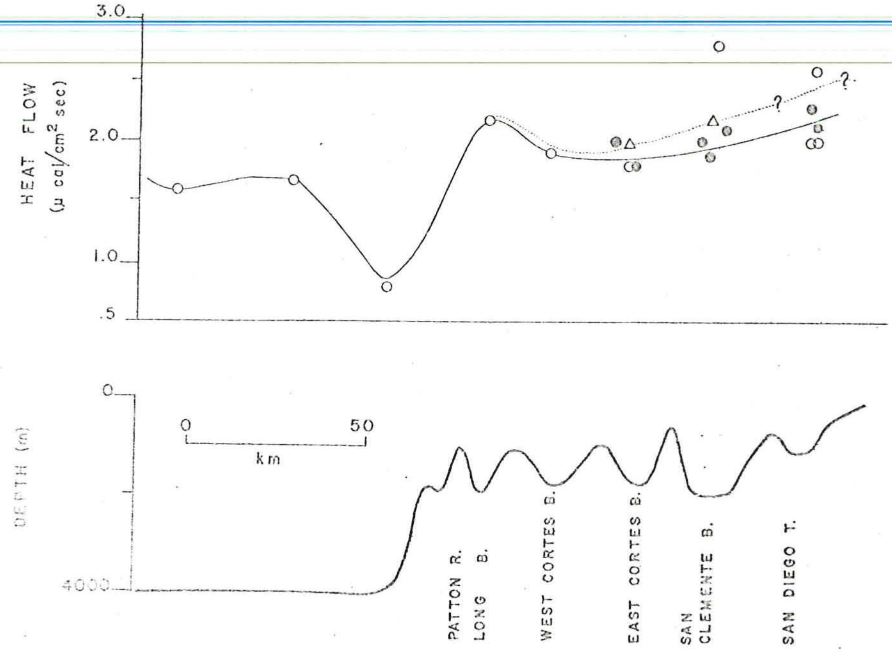

Fig. 9. Heat flow profile III-III′ across the strike of regional structure.

migrating heat source, the increase in heat flow to the southeast can be explained.

The geographic distribution of heat flow data revealed in this study may impose a significant constraint on the tectonic modeling of the borderland. The borderland is believed to have been affected by regional strike slip movement due to the interaction of the Pacific and American plates and may also have responded to the opening of the Gulf of California with local and regional rifting. A tectonic model for the formation of the borderland should incorporate the implications from the heat flow data that the borderland was formed progressively from northwest to southeast and that the development of offshore basins proceeded landward.

APPENDIX

Temporal variation of paleotemperature at a given locality, especially in the marine environment, is often expressed as a set of linear segments connecting discretely determined data points. Here we derive a solution to estimate the effect of temperature variation on geothermal gradient.

Consider the case that the semi-infinite region $z \geq 0$ is initially at temperature $G + gz$ and the plane $z = 0$ is maintained

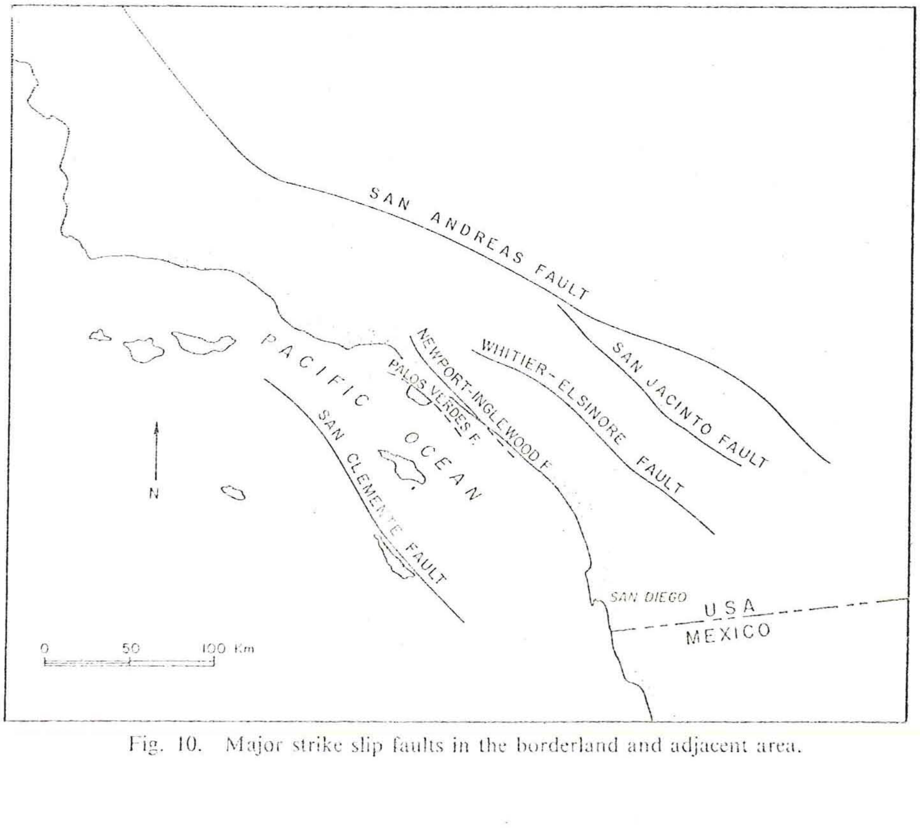

Fig. 10. Major strike slip faults in the borderland and adjacent area.

at $\phi(t)$ for time $t \geq T_0$. The temperature V is governed by

$$\frac{\partial V}{\partial t} = \alpha \frac{\partial^2 V}{\partial z^2} \tag{1}$$

$$V = G + gz \qquad t \leq T_0 \tag{2}$$

and

$$V = \phi(t) \qquad z = 0 \tag{3}$$

where α is the thermal diffusivity of the medium. The solution V can be obtained from a combination of u and w, i.e.,

$$V = u + w \tag{4}$$

if

$$\begin{aligned} \frac{\partial u}{\partial t} &= \alpha \frac{\partial^2 u}{\partial z^2} \\ u &= 0 \qquad t \leq T_0 \\ u &= \phi(t) \qquad z = 0 \end{aligned} \tag{5}$$

and

$$\begin{aligned} \frac{\partial w}{\partial t} &= \alpha \frac{\partial^2 w}{\partial z^2} \\ w &= gz + G \qquad t \leq T_0 \\ w &= 0 \qquad z = 0 \end{aligned} \tag{6}$$

Solutions u and w are essentially the same as those given by *Carslaw and Jaeger* [1959, pp. 63, 61],

$$u(z, T) = \frac{z}{2(\pi\alpha)^{1/2}} \int_0^{T-T_0} \phi(\lambda) \frac{e^{-z^2/4\alpha(T-T_0-\lambda)}}{(T - T_0 - \lambda)^{3/2}} \, d\lambda \tag{7}$$

and

$$w(z, T) = gz + G \operatorname{erf} \left\{ \frac{z}{2[\alpha(T - T_0)]^{1/2}} \right\} \tag{8}$$

The spatial derivatives of u and w are

$$\begin{aligned} \frac{\partial u}{\partial z} = {} & \frac{1}{2(\pi\alpha)^{1/2}} \int_0^{T-T_0} \phi(\lambda) \frac{e^{-z^2/4\alpha(T-T_0-\lambda)}}{(T - T_0 - \lambda)^{3/2}} \, d\lambda \\ & - \frac{z^2}{4(\pi\alpha^3)^{1/2}} \int_0^{T-T_0} \phi(\lambda) \frac{e^{-z^2/4\alpha(T-T_0-\lambda)}}{(T - T_0 - \lambda)^{5/2}} \, d\lambda \end{aligned} \tag{9}$$

$$\frac{\partial w}{\partial z} = g + \frac{G}{[\pi\alpha(T - T_0)]^{1/2}} e^{-z^2/4\alpha(T-T_0)} \tag{10}$$

Now approximate the paleotemperature $\phi(t)$ by m linear segments, i.e.,

$$\phi_j(t) = a_j + b_j(t - t_j) \qquad t_j \leq t \leq t_{j+1} \tag{11}$$

where

$$a_{j+1} = a_j + b_j(t_{j+1} - t_j) \qquad j = 1, 2, \cdots, m \tag{12}$$

$$t_1 = T_0$$

and

$$t_{m+1} = T$$

Near the surface the perturbation from the undisturbed gradient is therefore

$$\begin{aligned} \left(\frac{\partial V}{\partial z}\right)_{z=0} - g = {} & \frac{G}{[\pi\alpha(T - T_0)]^{1/2}} + \frac{1}{2(\pi\alpha)^{1/2}} \\ & \cdot \int_0^{T-T_0} \frac{\phi(\lambda)}{(T - T_0 - \lambda)^{3/2}} \, d\lambda = \frac{G}{[\pi\alpha(T - T_0)]^{1/2}} \\ & + \frac{1}{2(\pi\alpha)^{1/2}} \sum_{j=1}^{m} \int_{t_j-T_0}^{t_{j+1}-T_0} \frac{a_j + b_j(\lambda - t_j)}{(T - T_0 - \lambda)^{3/2}} \, d\lambda \\ = {} & \frac{G}{[\pi\alpha(T - T_0)]^{1/2}} + \frac{1}{(\pi\alpha)^{1/2}} \sum_{j=1}^{m} \left[\frac{a_j + b_j(T - t_j)}{(T - \lambda)^{1/2}} \right. \\ & \left. + b_j(T - \lambda)^{1/2} \right] \Bigg|_{t_j}^{t_{j+1}} \end{aligned} \tag{13}$$

With regard to the present bottom water temperature, the first term in (13) represents the effect of a sudden temperature change at $t = T_0$. This effect is enhanced or subdued by subsequent bottom water temperature variations $a_j + b_j(t - t_j)$. The apparent singularity arising from the factor $(T - t)^{-1/2}$ at $t = t_m = T$ in fact does not exist since $a_m + b_m(T - t_m) = 0$.

Acknowledgments. This study was supported by the National Science Foundation grants GA 13008 and GA 30633. We are grateful to Richard P. Von Herzen for his comments on this manuscript and to Roger Anderson and Larry Lawver for their unpublished data. Field work has been assisted by the crew members of R/V *Velero IV*, D. Manov, E. Welday, and J. Combs. Contribution 343, Department of Geological Sciences, University of Southern California, Los Angeles, California 90007.

REFERENCES

Atwater, T., Implications of plate tectonics for the Cenozoic tectonic evolution of western North America, *Geol. Soc. Amer. Bull., 81,* 3513–3536, 1970.

Birch, F., Flow of heat in the Front Range, Colorado, *Geol. Soc. Amer. Bull., 61,* 567–630, 1950.

Carslaw, H. S., and J. C. Jaeger, *Conduction of Heat in Solids,* 510 pp., Oxford University Press, New York, 1959.

Doyle, L. J., Marine geology of the Baja California Continental Borderland, Mexico, Ph.D. dissertation, 193 pp., Univ. of S. Calif., Los Angeles, 1973.

Emery, K. O., *The Sea off Southern California, A Modern Habitat of Petroleum,* 366 pp., John Wiley, New York, 1960.

Emery, K. O., and E. E. Bray, Radiocarbon dating of California basin sediments, *Amer. Ass. Petrol. Geol. Bull., 46,* 1839–1856, 1962.

Foster, T. D., Heat flow measurements in the northeast Pacific and in the Bering Sea, *J. Geophys. Res., 67,* 2991–2993, 1962.

Gorsline, D. S., D. E. Drake, and P. W. Barnes, Holocene sedimentation in Tanner Basin, California Continental Borderland, *Geol. Soc. Amer. Bull., 79,* 659–674, 1968.

Gorsline, D. S., and P. W. Barnes, Carbonate variations as climatic indicators in contemporary California flysch basins, *Int. Geol. Congr., 24,* sec. 6, 270–277, 1972.

Henyey, T. L., and G. J. Wasserburg, Heat flow near major strike-slip faults in California, *J. Geophys. Res., 76,* 7924–7946, 1971.

Hill, M., Newport-Inglewood fault zone and Mesozoic subduction, California, *Geol. Soc. Amer. Bull., 82,* 2957–2962, 1971.

Inman, D. L., and E. D. Goldberg, Petrogenesis and depositional rates of sediments from experimental Mohole drilling off La Jolla, California, *Eos Trans. AGU, 44,* 68–69, 1963.

Jaeger, J. C., Application of the theory of heat conduction to geothermal measurements, in *Terrestrial Heat Flow, Monogr. Ser.,* vol. 8, edited by W. H. K. Lee, pp. 7–23, AGU, Washington, D. C., 1965.

Jahns, R. H., Geology of the Peninsular Range province, southern California and Baja California, in *Geology of Southern California, Calif. Div. Mines Geol. Bull., 170,* 29–52, 1954.

Krause, D. O., Tectonics, bathymetry and geomagnetism of the southern Continental Borderland west of Baja California, Mexico, *Geol. Soc. Amer. Bull., 76,* 617–650, 1965.

Lachenbruch, A. H., and J. H. Sass, Thermo-mechanical aspects of the San Andreas fault system, *Stanford Univ. Publ. Univ. Ser. Geol. Sci.*, *13*, 192–205, 1973.

Langseth, M. G., Techniques of measuring heat flow through the ocean floor, *Terrestrial Heat Flow, Monogr. Ser.*, vol. 8, edited by W. H. K. Lee, pp. 58–77, AGU, Washington, D. C., 1965.

Lawver, L. A., J. G. Sclater, T. L. Henyey, and J. Rogers, Heat flow measurements in the southern portion of the Gulf of California, *Earth Planet. Sci. Lett.*, *19*, 198–208, 1973.

Lee, T. C., Heat flow and other geophysical studies in the southern California borderland, Ph.D. dissertation, 332 pp., Univ. of S. Calif., Los Angeles, 1973.

Menard, H. W., Deformation of the northeastern Pacific Basin and the west coast of North America, *Geol. Soc. Amer. Bull.*, *66*, 1149–1198, 1955.

Moore, D. G., Reflection profiling studies of the California Continental Borderland, Structure and Quaternary turbidites basins, *Geol. Soc. Amer. Spec. Pap. 107*, 142 pp., 1969.

Ratcliffe, E. H., The thermal conductivities of ocean sediments, *J. Geophys. Res.*, *65*, 1535–1541, 1960.

Rittenberg, S. C., K. O. Emery, and W. L. Orr, Regeneration of nutrients in sediments of marine basins, *Deep Sea Res.*, *3*, 23–45, 1955.

Roy, R. F., D. D. Blackwell, and F. Birch, Heat generation of plutonic rocks and continental heat flow provinces, *Earth Planet. Sci. Lett.*, *5*, 1–12, 1968.

Roy, R. F., D. D. Blackwell, and E. R. Decker, Continental heat flow, in *Nature of the Earth*, edited by E. D. Robertson, J. F. Hays, and L. Knopoff, 677 pp., McGraw-Hill, New York, 1972.

Roy, R. F., J. Brune, C. Lomnitz, and F. Mooser, Heat flow in Baja California and western Mexico, *Geol. Soc. Amer. Abstr. Program*, *5*, 98, 1973.

Sass, J. H., A. H. Lachenbruch, R. J. Munroe, G. W. Green, and T. H. Moses, Jr., Heat flow in the western United States, *J. Geophys. Res.*, *76*, 6376–6413, 1971.

Sclater, J. G., and J. Francheteau, The implications of terrestrial heat flow observations on current tectonic and geochemical models of the crust and the upper mantle of the earth, *Geophys. J.*, *20*, 509–542, 1970.

Shepard, F. E., and K. O. Emery, Submarine topography off the California coast: Canyons and tectonic interpretation, *Geol. Soc. Amer. Spec. Pap. 31*, 171 pp., 1941.

Shor, G. G., and R. W. Raitt, Seismic studies in the southern California borderland, *Congr. Geol. Int.*, 243–259, 1958.

Sverdrup, H. U., M. W. Johnson, and R. H. Fleming, *The Ocean*, Prentice-Hall, Englewood Cliffs, N. J., 1942.

Von Herzen, R. P., and A. E. Maxwell, The measurement of thermal conductivity of deep sea sediments by a needle probe method, *J. Geophys. Res.*, *64*, 1557–1565, 1959.

Von Herzen, R. P., and S. Uyeda, Heat flow through the eastern Pacific Ocean floor, *J. Geophys. Res.*, *68*, 4219–4250, 1963.

Von Herzen, R. P., Ocean floor heat-flow measurements west of the United States and Baja California, *Mar. Geol.*, *1*, 225–239, 1964.

Yeats, R. S., Rifting and rafting in the southern California borderland, *Stanford Univ. Pubs. Univ. Ser. Geol. Sci.*, *11*, 144–165, 1968.

Yeats, R. S., M. R. Cole, W. R. Merschat, and R. M. Parsley, Poway fan and submarine cone and rifting of the inner southern California borderland, *Geol. Soc. Amer. Bull.*, *85*, 293–302, 1974.

Yerkes, R. F., T. H. McCulloh, J. E. Schoellhamer, and J. G. Vedder, Geology of the Los Angeles basin—An introduction, *U.S. Geol. Surv. Prof. Pap. 420A*, 57 pp., 1965.

(Received December 5, 1974;
revised April 7, 1975;
accepted April 10, 1975.)